arXiv:1403.7590v1 [cond-mat.supr-con] 29 Mar 2014

Raman scattering investigation of superconducting $Ba_2Ti_2Fe_2As_4O$

S. -F. Wu,[1] P. Richard,[1,2,*] W. -L. Zhang,[1] C. -S. Lian,[1] Y. -L. Sun,[3] G. -H. Cao,[3] J. -T. Wang,[1] and H. Ding[1,2,†]

[1] *Beijing National Laboratory for Condensed Matter Physics, and Institute of Physics, Chinese Academy of Sciences, Beijing 100190, China*

[2] *Collaborative Innovation Center of Quantum Matter, Beijing, China*

[3] *Department of Physics, State Key Lab of Silicon Materials, and Center of Electron Microscopy, Zhejiang University, Hangzhou 310027, China*

(Dated: April 1, 2014)

We have performed polarized Raman scattering measurements on the newly discovered superconductor $Ba_2Ti_2Fe_2As_4O_2$ (T_c = 21 K). We observe seven out of eight Raman active modes, with frequencies in good accordance with first-principle calculations. The phonon spectra suggest neither strong electron-phonon nor spin-phonon coupling and vary only slightly with temperature, except for one E_g mode associated with large displacements of As atoms near the Ti_2O planes. We also identify a small anomaly around 125 K in the linewidth of a A_{1g} mode involving the same As atoms. Our results suggest that the transition at 125 K is most likely driven by electronic interactions taking place in the Ti_2O planes.

PACS numbers: 74.70.Xa, 74.25.nd, 74.25.Kc

Despite a low superconducting critical temperature (T_c) of 1.2 K [1], $BaTi_2Sb_2O$ is widely regarded as a possible candidate for unconventional superconductivity. Indeed, its square Ti_2O layers with a Ti $3d^1$ electron shell are quite similar to the CuO_2 layers with a Cu $3d^9$ electron shell of the high-T_c cuprate superconductors. Interestingly, this material exhibits an anomaly in the electrical resistivity at a temperature T_a = 50 K, which is attributed either to a charge-density-wave (CDW) or a spin-density-wave (SDW). The observation of similar anomalies at 200 K and 114 K in non-superconducting $BaTi_2As_2O$ [2] and $Na_2Ti_2Sb_2O$ [3], and its disappearance in Na-doped $Ba_{1-x}Na_xTi_2Sb_2O$ with an enhanced T_c of 5.5 K [4], suggest a competition between superconductivity and the CDW/SDW order. Interest for this topic raised even further with the recent discovery of $Ba_2Ti_2Fe_2As_4O$ with T_c = 21 K [5], which is an intergrowth of $BaTi_2As_2O$ and $BaFe_2As_2$, the parent compound of the 122 family of ferropnictide superconductors. For this material, a transition at 125 K has been identified from the electrical resistivity and the magnetic susceptibility. Unfortunately, whether this transition is related to a CDW or a SDW is still under debate.

In this paper, we use Raman scattering to investigate directly the crystallographic structure of $Ba_2Ti_2Fe_2As_4O$. We observed seven out of eight Raman active modes, with frequencies in good accordance with first-principle calculations. The phonon spectra suggest neither strong electron-phonon nor spin-phonon coupling and vary only slightly with temperature, except for a 11 cm^{-1} shift observed for one E_g mode involving large displacements of As atoms near the Ti_2O. Our analysis of the phonon linewidths also revealed a small anomaly around T_a = 125 K for a A_{1g} mode involving the same As atoms. Our results suggest that the transition at T_a is of electronic nature and originates from the Ti_2O planes.

The $Ba_2Ti_2Fe_2As_4O$ single crystals used in our Raman scattering measurements were grown by solid-state reactions [5]. The resistivity of the samples was measured with a Quantum Design physical properties measurement system (PPMS), and the magnetization of the samples was measured with a vibrating sample magnetometer (VSM). The magnetization measurements show that only about 30-40% of the volume was superconducting, suggesting inhomogeneous superconductivity. The crystals were cleaved in air to obtain flat surfaces and then transferred into a low-temperature cryostat ST500 (Janis) for the Raman measurements between 5 and 300 K with a working vacuum better than 8×10^{-7} mbar. Raman scattering measurements were performed using 488.0 nm, 514.5 nm and 647.1 nm laser lines in a back-scattering micro-Raman configuration with a triple-grating spectrometer (Horiba Jobin Yvon T64000) equipped with a nitrogen-cooled CCD camera. In this manuscript, we define x and y as the directions along the a and b axes, oriented at 45° from the Fe-Fe bounds, and x' and y' as the directions along the Fe-Fe bounds. The z direction corresponds to the c-axis perpendicular to the FeAs and TiO_2 planes.

The $Ba_2Ti_2Fe_2As_4O$ crystal structure is characterized by the space group D_{4h}^{17} (I4/mmm). A simple group symmetry analysis [6] indicates that the phonon modes at the Brillouin zone (BZ) center decompose into $[3A_{1g}+B_{1g}+4E_g]+[5A_{2u}+B_{2u}+6E_u]+[A_{2u}+E_u]$, where the first, second and third terms represent the Raman-active modes, the infrared(IR)-active modes and the acoustic modes, respectively. To get estimates on the phonon frequencies, we performed first-principle calculations in the non-magnetic phase of the phonon modes at the BZ center in the framework of the density functional perturbation theory (DFPT) [7], using the experimental lattice parameters $a = b$ = 4.0276 Å and c = 27.344 Å,

* p.richard@iphy.ac.cn
† dingh@iphy.ac.cn

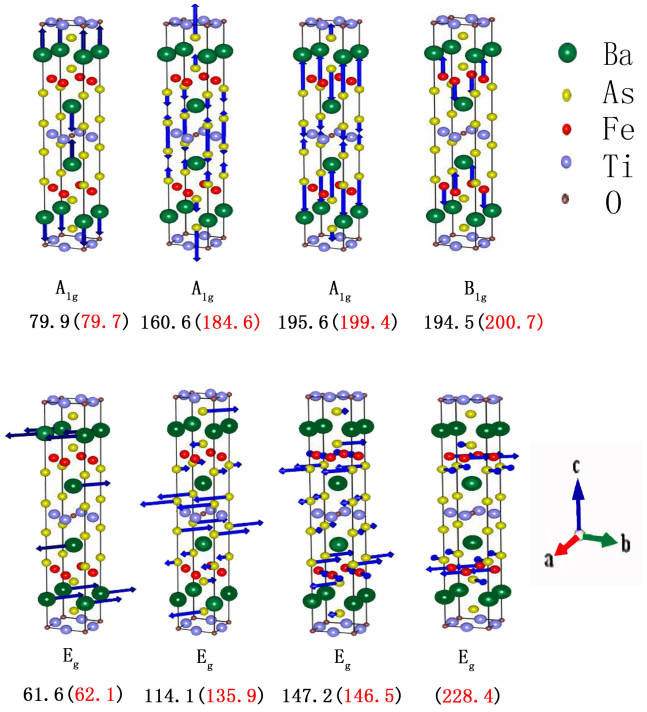

FIG. 1. (Color online). Atomic displacement patterns for the eight Raman-active modes of $Ba_2Ti_2Fe_2As_4O$. The values in black correspond to the experimental values while the ones in red, inside brackets, are the calculated values.

and the Wyckoff positions Ba 2i, Ti 4e, Fe 2i, As 2i, O 4e. For all calculations, we used the Vienna *ab initio* simulation package (VASP) [8] with the generalized gradient approximation (GGA) of Perdew-Burke-Ernzerhof for the exchange-correlation functions [9]. The projector augmented wave (PAW) [10] method was employed to describe the electron-ion interactions. A plane wave cutoff energy of 520 eV was used with a uniform $9\times9\times9$ Monkhorst-Pack k-point mesh for integrations over the BZ. The frequencies and displacement patterns of the phonon modes were derived from the dynamical matrix generated by the DFPT method. The calculated frequencies and the optical activity of the phonon modes are given in Table I, and the atomic displacements of the Raman-active phonon modes are illustrated in Fig. 1.

In Figs. 2(a) and 2(b), we show the Raman spectra of $Ba_2Ti_2Fe_2As_4O$ recorded at room temperature under various polarization configurations. The symmetry of the modes observed are determined by the Raman tensors corresponding to the D_{4h} symmetry group, which are expressed as:

$$A_{1g}=\begin{pmatrix} a & 0 & 0\\ 0 & a & 0\\ 0 & 0 & b\end{pmatrix}, B_{1g}=\begin{pmatrix} c & 0 & 0\\ 0 & -c & 0\\ 0 & 0 & 0\end{pmatrix},$$

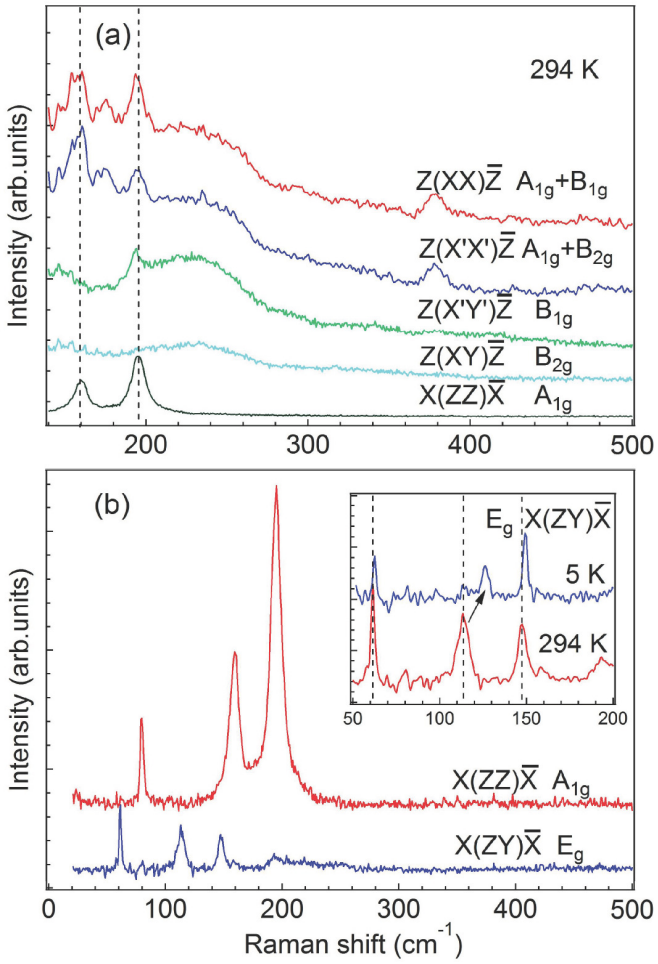

FIG. 2. (Color online). (a) Polarization dependence of the *ab* plane measurements of $Ba_2Ti_2Fe_2As_4O$ at 294 K. (b) Polarization dependence of the *ac* plane measurements at 294 K. The inset compares the Raman spectra recorded at 294 K in the E_g channel. The vertical dashed lines in (a) and in the inset of panel (b) are guides to the eye while the small arrow in the inset indicates a peak shift.

$$B_{2g}=\begin{pmatrix} 0 & d & 0\\ d & 0 & 0\\ 0 & 0 & 0\end{pmatrix}, E_g=\left\{\begin{pmatrix} 0 & 0 & 0\\ 0 & 0 & e\\ 0 & e & 0\end{pmatrix}, \begin{pmatrix} 0 & 0 & -e\\ 0 & 0 & 0\\ -e & 0 & 0\end{pmatrix}\right\}.$$

For perfectly aligned crystals, pure A_{1g} symmetry is obtained in the $x(zz)\bar{x}$ configuration. In this channel, we detect 3 sharp peaks at 79.7 cm^{-1}, 160.6 cm^{-1} and 195.6 cm^{-1}. As illustrated in Fig. 1, they correspond to c-axis vibrations of the Ba atoms, As atoms in near the Ti_2O layer (As^1) and As atoms in the Fe-As layer (As^2), respectively. In Fig. 2(a), we show that the A_{1g} peaks survive in the $z(xx)\bar{z}$ and $z(x'x')\bar{z}$ configurations, for which the A_{1g} signal is mixed with signals from the B_{1g} and B_{2g} channels, respectively.

In agreement with our group analysis, no phonon peak is detected in the $z(xy)\bar{z}$ configuration, which corresponds to pure B_{2g} symmetry. However, we observe a

broad hump at 230 cm^{-1} that appears in the four in-plane polarization configurations but disappears in the ac plane measurements, and which we relate to impurities or inhomogeneity. In addition to that peak, a phonon peak is detected at 194.5 cm^{-1} in the $z(x'y')\bar{z}$ configuration corresponding to pure B_{1g} symmetry. Although that peak is located almost at the same position as one of the A_{1g} peaks, several arguments suggest that these two features might have different origins. In principle, A_{1g} peaks should be detected only in configurations for which the polarization vectors of the incident and scattered lights are parallel, which is not the case for both the B_{1g} and B_{2g} configurations. In addition, if the presence of a A_{1g} peak in the B_{1g} spectrum was due to misalignment, the same peak should also appear in the B_{2g} spectrum, in contrast to our results. Moreover, according to our calculations, the energy of the B_{1g} mode corresponding to vibrations of the Fe atoms along the c axis is similar to that of one A_{1g} mode.

Finally, three out of four E_g modes are detected in the $x(zy)\bar{x}$ polarization configuration spectrum shown in Fig. 2(b). As illustrated in Fig. 1, the E_g modes found experimentally at 61.6 cm^{-1}, 114.1 cm^{-1} and 147.2 cm^{-1} are associated with in-plane motions of Ba atoms, As^1 atoms near the Ti_2O layer and As^2 atoms in the Fe-As layer, respectively. Besides the regular Raman-active phonon peaks observed (7 out of 8 modes) and the hump at 230 cm^{-1} mentioned above, we observe small peaks at 175 cm^{-1} and at 380 cm^{-1} in both the $z(xx)\bar{z}$ and $z(x'x')\bar{z}$ configurations, which we cannot assign. Indeed, these peaks do not follow the selection rules corresponding to $Ba_2Ti_2Fe_2As_4O$ and we thus suspect that they come from an impurity phase, our samples containing 7.5% of them [5].

To investigate the possible role of the lattice on the density-wave transition at $T_a = 125$ K and on the superconducting transition at $T_c = 21$ K, we cooled the samples down to 5 K. In Fig. 3(a), we display the temperature dependence of the A_{1g} peaks at 160.6 cm^{-1} and 195.6 cm^{-1}. As expected, the peaks become a little sharper with temperature decreasing. The symmetric Lorentzian lineshapes at all temperatures suggest that there is neither strong electron-phonon coupling nor spin-phonon coupling in this system. In contrast with our expectation for a CDW transition, the peak positions barely change with temperature. We show in Figs. 3(b) and 3(c) a quantitative analysis of the peak position and the linewidth of the A_{1g} Raman peak at 159.0 cm^{-1}, which has been fit simultaneously with two Lorentzian functions convoluted by a Gaussian function representing the system resolution. The peak position $\omega_{ph}(T)$ and the linewidth $\Gamma_{ph}(T)$ follow simple expressions corresponding to the anharmonic phonon decay into acoustic phonons with the same frequencies and opposite momenta [11, 12]:

$$\omega_{ph}(T) = \omega_0 - C\left(1 + \frac{2}{e^{\frac{\hbar\omega_0}{2k_BT}} - 1}\right) \qquad (1)$$

TABLE I. Comparison of the calculated and experimental phonon modes at 294 K.

Sym.	Act.	Exp.	Cal.	Main atom displacements
E_u	IR		51.7	Ti(xy), As^1(xy), Fe(-xy), As^2(xy)
E_g	Raman	61.6	62.1	Ba(xy)
A_{2u}	IR		69.3	O(z), As^1(z)
A_{1g}	Raman	79.9	79.7	Ba(z)
E_u	IR		84.9	Ba(xy)
A_{2u}	IR		87.9	Ba(z), Fe(z), As^2(z)
E_g	Raman	114.1	135.9	As^1(xy)
E_g	Raman	147.2	146.5	As^2(xy)
E_u	IR		165.8	Ti(xy), As^1(-xy)
B_{2u}	IR		178.5	Ti(z)
A_{1g}	Raman	160.6	184.6	As^1(z)
A_{2u}	IR		190.0	As^2(z), O(-z)
A_{1g}	Raman	195.6	199.4	As^2(z)
B_{1g}	Raman	194.5	200.7	Fe(z)
E_u	IR		226.4	Ti(xy), O(-xy)
E_g	Raman	-	228.4	Fe(xy), As^2(xy)
A_{2u}	IR		246.4	Ti(z), As^1(-z)
A_{2u}	IR		259.5	Fe(z), As(-z)
E_u	IR		274.5	Fe(xy), As(xy)
E_u	IR		546.1	Ti(xy), O(-xy)

As^1 next to the Ti_2O layer; As^2 Fe-As layer

$$\Gamma_{ph}(T) = \Gamma_0 + \Gamma\left(1 + \frac{2}{e^{\frac{\hbar\omega_0}{2k_BT}} - 1}\right), \qquad (2)$$

where C and Γ are positive constants, ω_0 is the bare phonon frequency, and Γ_0 is a residual, temperature-independent linewidth. From the fit, we extract $\omega_0 = 163.1$ cm^{-1}, $C = 0.787$ cm^{-1}, $\Gamma = 5.00$ cm^{-1} and $\Gamma_0 = 1.89$ cm^{-1}. Similarly, The position of the A_{1g} peak at 195.6 cm^{-1} is well fitted with the formulas with $\omega_0 = 200.5$ cm^{-1}, $C = 1.353$ cm^{-1}, $\Gamma = 4.07$ cm^{-1} and $\Gamma_0 = 2.20$ cm^{-1}. However, it is not possible to fit the linewidth of this peak with Eq. (2), an increase in the slope while cooling down occurring around $T_a = 125$ K, as shown in Fig. 3(e).

Our results indicate that neither the phonon peak positions nor the phonon linewidths are affected by the superconducting transition at $T_c = 21$ K. Similar behaviors have been reported in Raman studies on $NdFe_2As_2O_{1-x}F_x$ [13, 14], $Sr_{1-x}K_xFe_2As_2$ and $Ba_{1-x}K_xFe_2As_2$ [15–17], and on $Ba(Fe_{1-x}Co_x)_2As_2$ [18]. On the other hand, anomalies in the peak positions and in the phonon linewidths across the SDW transition have been evidenced in previous Raman studies of $BaFe_2As_2$ [16], $CaFe_2As_2$ [19] and FeTe [20], as well as the splitting of a doubly-degenerate E_g mode [18] due to the breakdown of the four-fold symmetry accompanying this transition. In contrast, we do not observe any anomaly in the temperature evolution of the peak position of the phonons of $Ba_2Ti_2Fe_2As_4O_2$, and only a small anomaly

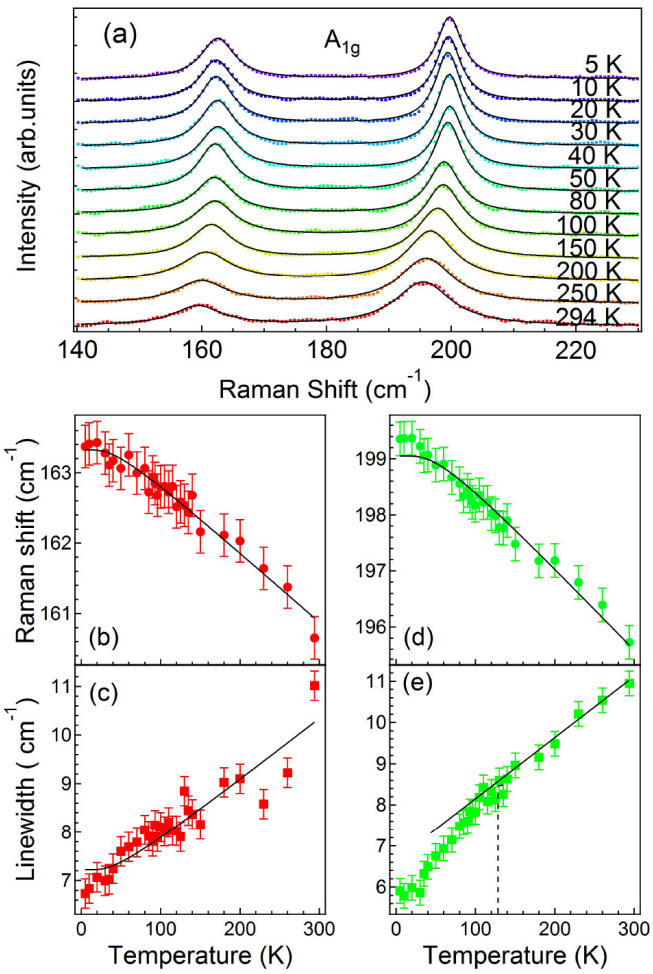

FIG. 3. (Color online). (a) Temperature dependence of the Raman spectra for the A_{1g} modes at 160.6 cm^{-1} and 195.6 cm^{-1}. The black lines represent the fit curves. (b)-(c) Peak position and linewidth (full width at half maximum), respectively, of the A_{1g} mode at 160.6 cm^{-1}. (d)-(e) Same as (b)-(c) but for the the A_{1g} mode at 160.6 cm^{-1}. The curves in (b)-(d) are fit to the equations Eqs. (1) and (2). The dashed lines in (e) are guides to the eye for an anomaly around 125 K.

is observed around $T_a = 125$ K in the linewidth of the phonon at 195.6 cm^{-1}, as shown in Fig. 3(e). This suggests that the transition at T_a is only weakly coupled to the lattice and is most likely from pure electronic origin, which is supported by a spectral weight transfer from the Drude peak to about 800 cm^{-1} in the optical conductivity of the same material across the transition [21]. This is also consistent with muon spin relaxation measurements on $BaTi_2(As_{1-x}Sb_x)_2O$ suggesting the absence of atomic modulation across T_a [22].

In contrast to the SDW transition found in several Fe-based superconductors, which breaks the four-fold symmetry, we observe no indication of such a symmetry lowering around T_a in $Ba_2Ti_2Fe_2As_4O_2$ that could produce a splitting of the E_g modes, as shown in the inset of Fig. 2(b). Actually, the position of the modes at 61.6 cm^{-1} and 147.2 cm^{-1} barely changes with temperature. Interestingly, only the mode at 114.1 cm^{-1} exhibits a large energy shift as compare to all the other phonon peaks, and is detected at 125 cm^{-1} at 5 K. This is possibly due to a strong coupling between this mode and the transition at T_a. As illustrated in Fig. 1, this E_g mode involves large displacements of the As^1 atoms in close proximity to the Ti atoms. Consistently, the A_{1g} mode at 195.6 cm^{-1} showing a linewidth anomaly around T_a also involves the As^1 atoms. This suggests that the transition at T_a most likely occurs due to electronic interactions in the Ti_2O planes, and that its origin would be closely related to the one found in Fe-free $BaTi_2As_2O$ [2] and $Na_2Ti_2Sb_2O$ [3]. Although more experimental work using probes directly sensitive to the element selective electronic structure is necessary to validate this hypothesis, our work already provides a clear indication that the transition has a purely electronic origin.

In summary, we have performed polarized Raman scattering measurements on the newly discovered superconductor $Ba_2Ti_2Fe_2As_4O_2$ ($T_c = 21$ K). We observe seven out of eight Raman active modes, with frequencies in good accordance with first-principle calculations. The phonon spectra suggest neither strong electron-phonon nor spin-phonon coupling and vary only slightly with temperature, at the exception of an E_g mode involving large displacements of As atoms in the vicinity of the Ti_2O planes. We also report a small anomaly around T_a in the linewidth of an A_{1g} mode also involving As atoms in the vicinity of the Ti_2O planes. Our results suggest that the transition at T_a originates from electronic interactions in the Ti_2O planes.

We acknowledge H. Miao and J. -X. Yin for useful discussions. This work was supported by grants from CAS (2010Y1JB6), MOST (2010CB923000, 2011CBA001000, 2011CBA00102, 2012CB821403 and 2013CB921703) and NSFC (11004232, 11034011/A0402, 11234014 and 11274362) from China.

[1] T. Yajima, K. Nakano, F. Takeiri, T. Ono, Y. Hosokoshi, Y. Matsushita, J. Hester, Y. Kobayashi and H. Kageyama, J. Phys. Soc. Jpn. **81**, 103706 (2012).
[2] X. F. Wang, Y. J. Yan, J. J. Ying, Q. J. Li, M. Zhang, N. Xu and X. H. Chen, J. Phys: Condens. Matter **22**, 075702 (2010).
[3] A. Adam and H.-U. Schuster, Z. Anorg. Allg. Chem. **584**, 150 (1990).
[4] P. Doan, M. Gooch, Z. Tang, B. Lorenz, A. Möller, J. Tapp, P. C. W. Chu and A. M. Guloy, J. Am. Chem. Soc. **134**, 16520 (2012).
[5] Y.-L. Sun, H. Jiang, H.-F. Zhai, J.-K. Bao, W.-H. Jiao,

Q. Tao, C.-Y. Shen, Y.-W. Zeng, Z.-A. Xu and G.-H. Cao, J. Am. Chem. Soc. **134**, 12893 (2012).
[6] E. Coumarou, M. I. Arroyo, J. M. Perez Cato, A. Kirov, C. Candelillas, S. Revanche and H. Chandrasekhar, Phase Transitions **76**, 155 (2003).
[7] S. Baroni, S. de Gironcoli, A. Dal Corso and P. Giannozzi, Rev. Mod. Phys. **73**, 515 (2001).
[8] G. Kresse and J. Furthmüller, J. Phys. C **54**, 11169 (1996).
[9] J. P. Perdew and Y. Wang, Phys. Rev. B **46**, 6671 (1992).
[10] P. E. Blöchl, Rev. Mod. Phys. **50**, 17953 (1994).
[11] P. G. Klemens, Phys. Rev. **148**, 845 (1966).
[12] J. Menéndez and M. Cardona, Phys. Rev. B **29**, 2051 (1984).
[13] Y. Gallais, A. Sacuto, M. Cazayous, P. Cheng, L. Fang, and H. H. Wen, Phys. Rev. B **78**, 132509 (2008).
[14] L. Zhang, T. Fujita, F. Chen, D. L. Feng, S. Maekawa, and M. W. Chen, Phys. Rev. B **79**, 052507 (2009).
[15] A. P. Litvinchuk, V. G. Hadjiev, M. N. Iliev, B. Lv, A. M. Guloy, and C. W. Chu, Phys. Rev. B **78**, 060503 (2008).
[16] M. Rahlenbeck, G. L. Sun, D. L. Sun, C. T. Lin, B. Keimer, and C. Ulrich, Phys. Rev. B **80**, 064509 (2009).
[17] K.-Y. Choi, P. Lemmens, I. Eremin, G. Zwicknagl, H. Berger, G. L. Sun, D. L. Sun and C. T. Lin, J. Phys.: Condens. Matter **22**, 115802 (2010).
[18] L. Chauvière, Y. Gallais, M. Cazayous, A. Sacuto, M. A. Méasson, D. Colson, and A. Forget, Phys. Rev. B **80**, 094504 (2009).
[19] K.-Y. Choi, D. Wulferding, P. Lemmens, N. Ni, S. L. Bud'ko, and P. C. Canfield, Phys. Rev. B **78**, 212503 (2008).
[20] V. Gnezdilov, Y. Pashkevich, P. Lemmens, A. Gusev, K. Lamonova, T. Shevtsova, I. Vitebskiy, O. Afanasiev, S. Gnatchenko, V. Tsurkan, J. Deisenhofer, and A. Loidl, Phys. Rev. B **83**, 245127 (2011).
[21] H. P. Wang, Y.-L. Sun, G.-H. Cao, and N. L. Wang, Unpublished (2014).
[22] Y. Nozaki, K. Nakano, T. Yajima, H. Kageyama, B. Frandsen, L. Liu, S. Cheung, T. Goko, Y. J. Uemura, T. S. J. Munsie, T. Medina, G. M. Luke, J. Munevar, D. Nishio-Hamane and C. M. Brown, Phys. Rev. B **88**, 214506 (2013).